# E-Go Bicycle Intelligent Speed Adaptation System for Catching the Green Light

Khalil Ben Fredj(✉), Akhil Reddy Pallamreddy, Geert Heijenk, Paul Havinga, and Yanqiu Huang

Centre for Networked Systems and Intelligence, University of Twente, Enschede 7522 NB, The Netherlands
{k.benfredj,a.r.pallamreddy,geert.heijenk, p.j.m.havinga,yanqiu.huang}@utwente.nl

**Abstract.** The expanding growth of electric bikes in recent years underscores their increasing importance as a sustainable and eco-friendly mode of transportation. With zero emissions and the ability to ease urban congestion, e-bikes are becoming a pivotal solution in promoting greener and more efficient commuting habits. However, signalized intersections and frequent stops at traffic lights (TL) are considered uncomfortable for cyclists. This article introduces a personalized and privacy-preserving Intelligent Speed Adaption (ISA) system that helps cyclists adapt to the required speed to catch the green light. In our system design, traffic lights are augmented with Bluetooth Low Energy (BLE) beaconing devices which allow connected e-bikes to get the remaining green light phase duration, estimate the distance to the intersection, and assist the cyclist to catch the green light when necessary. We address the speed adaption problem as a convex optimization problem to ensure smooth and safe acceleration. In addition, a fuzzy logic controller is used to control motor power to reach the recommended speed while considering the human pedal power. We generate different scenarios with various initial velocities, time to red (TTR), slope of the road, and human pedal power to evaluate the system's performance. The results demonstrate that ISA improves the probability of crossing the traffic light by about 77% compared to the absence of speed adaptation.

**Keywords:** Smart e-bikes · Intelligent Speed Adaptation · Privacy Preserving · Fuzzy Logic Control · Bluetooth Low Energy · RSSI distance estimation · SPaT

## 1 Introduction

Bicycles are essential in our daily lives as a sustainable, affordable, and healthy mode of transportation [7]. Cycling not only provides a viable alternative to cars, reducing traffic congestion and air pollution, but also helps to improve


A. Zaslavsky et al. (Eds.): MobiQuitous 2023, LNICST 593, pp. 201–220, 2024.
https://doi.org/10.1007/978-3-031-63989-0_10

public health, reducing the risk of chronic diseases associated with a sedentary lifestyle [11]. However, cycling in urban areas is inconvenient because the traffic infrastructure is designed primarily for cars [15]. Cyclists have prolonged waiting times at traffic intersections due to TL [22]. In addition, they often have difficulties in catching the green light because the time allotted for bicycles to cross an intersection is much shorter than the time allocated to cars. As a result, cyclists must be quick to start pedaling and often have to travel faster than a comfortable pace to get through before the traffic light turns red.

Municipalities, researchers, and industry players have developed innovative approaches to address this problem, such as sensor-based smart traffic lights and smartphone application-based systems [1,4]. Worldwide, functioning smart traffic light systems are available, particularly in The Netherlands, where the government has installed intelligent traffic lights capable of communicating with vehicles and navigation applications [2]. These smart traffic lights use reactive algorithms and data from various sensors (radar, LiDAR, camera, pressing button, and induction loop) to dynamically adjust signal phase and timing (SPaT) based on the volume of vehicles/cyclists at intersections. However, these systems require abundant infrastructure and lack personalization for safety and comfort.

In contrast, more personalized smart systems adapting to traffic lights rely on smartphone Apps like "PrioBike," "Schwung," and "Enschede fietst app" [1,3,4]. These applications use green light time predictions and cyclists' smartphone data (position, direction, and speed) to offer speed recommendations. Third-party developers collect TL data from local agencies and analyze them alongside cyclists' private data (GPS location, directions, speed) using time series prediction methods (e.g., LSTM and 1D-CNN). For example, to give a speed recommendation, the Green Light Optimal Speed Advisory (GLOSA) system estimates the distance between the TL and the bicycle from the GPS location of the bicycle and the location information received from the TL [24]. However, these systems have limited availability based on data-sharing agreements and require continuous user tracking for speed recommendations. While both sensor-based smart traffic lights and smartphone application-based systems have shown promising results, there is a need for a decentralized and anonymous local information-based solution.

In this work, the authors aim to address this limitation by considering dynamic expected velocities based on the distance to the traffic light, human pedal power, road slope, and time-to-red (TTR), ensuring appropriate motor power adjustments for efficient and safe cycling. This study establishes a personalized and privacy-preserving intelligent system that allows cyclists to catch green lights while maintaining comfort and safety. Usually, when cyclists approach the traffic light and see that it is green, they try to accelerate to cross the intersection before the TL turns red. However, they do not have information about the remaining green time. Consequently, either they put an unnecessary effort and cross the green light before it turns to red or the green phase duration is so short that they end up violating the red light. Assisting the cyclist to safely accelerate to the required speed when possible by catching the current green light phase will ensure safety and comfort.

The main contributions of this work include the following:

- This is the first work combining Bluetooth Low Energy (BLE) communication with the fuzzy logic controller-based motor power control system to adapt the bicycle speed for catching the green light.
- It formulates the speed adaptation problem as a convex optimization problem and provides the optimal strategy for controlling motor power to catch the green light while ensuring safety and comfort, which goes beyond the current state-of-the-art.
- The system in this work dynamically updates and enhances the distance estimates along the journey using a Kalman filter and the continuously received beacons from the TL, which is simple and preserves users' privacy compared to GPS-based solutions.

The paper is organized as follows. Section 2 introduces related work on motor power control and distance estimation methods. The system modeling and problem formulation are presented in Sect. 3. In Sect. 4, we provide the proposed speed adaptation system consisting of distance estimation and speed adaptation. The experimental and numerical results are illustrated in Sect. 5 followed by the discussion and future work in Sect. 6 and conclusion in Sect. 7.

## 2 Related Work

In this section, we present an overview of the present pinnacle of speed adaptation techniques aimed at effectively catching the green light. The manipulation of motor power in the bicycle's mechanics on the one hand, and the accurate estimation of distance between the e-bike and the traffic light on the other, constitute the pivotal components underpinning the functionality of the speed adaptation system. Consequently, we will explore separately the state of the art of the motor power control methods and the distance estimation techniques in the following two subsections.

### 2.1 Motor Power Control Methods

Thanks to several researchers, including [5,8,12,13,16–20,23,24] it is now possible to control the motor power in the bicycles to adapt their speed. So far, two types of assisted power methods are available for commercial electric-assist bicycles. The first is called constant-assisted power (CAP) [19]. It provides the rider with a consistent and predetermined level of power support, regardless of the pedal power applied. The second is proportional assisted power (PAP) [20]. The idea is to assist motor power proportionally to pedal power until a specific speed limit and then gradually recede. The limitations of these approaches are that they do not consider environmental factors contributing to the resistance (e.g., air drag, road surface friction), leading to tapering off the riding comfort and safety.

To address the problem of dealing with the different environmental circumstances that bicycles encounter a reinforcement learning (RL) based algorithm

is proposed in [13] to improve riding quality considering different road slopes and human pedal power. However, this RL-based solution requires abundant data and high computations, especially in dynamic environments for updating optimal policy to provide sufficient riding quality. To ensure riding quality, [5] proposed a sophisticated algorithm considering wind force and road slopes using a mixed controller to maintain a constant velocity, but its reliance on reliable inputs raises concerns in dynamic environments. To address the limitations posed from the above, a fuzzy logic controller (FLC) has been used to assist the cyclists [8,12,16–18,23,24]. The FLC demonstrates exceptional performance in dealing with vague and uncertain inputs and allows one to model and control complex systems in an intuitive and human-interpreted way. For example, Lee and Jiang [16] have proposed a solution that adapts the bicycle's speed by achieving the urban riding velocity (assuming the expected velocity to be 18 km/h throughout the journey) for ordinary, power-less, and powerful cyclists.

Although the results to date were prominent in maintaining comfort and safety throughout the journey, existing FLC-based methods can only adapt the speed to a predetermined constant velocity. In the real-time application realization, many factors affect the performance of the system, including stops in the TL. In order to catch the green light, the expected velocity should be dynamic along the journey, which depends on the distance to the TL, human pedal power, road slope, and TTR. Obtaining the dynamic expected velocity and adapting motor power accordingly remain overlooked. To the best of our knowledge, this is the first time that anyone has considered the dynamic change in the expected velocity for speed adaptation.

In this work, the authors aim to tackle this limitation by considering dynamic expected velocities based on the distance to the traffic light, human pedal power, road slope, and time-to-red (TTR), ensuring appropriate motor power adjustments for comfort and safe cycling.

### 2.2 Distance Estimation Methods

In order to find the dynamic expected velocity for crossing the traffic light, the distance between the bicycle and the TL is crucial to determine. The distance can be realized using positional information with Global Positioning System (GPS), sensors like camera, ultrasonic and LiDAR. One of the most used solutions for estimating the distance to the traffic light is GPS location information. For instance, in the Green Light Optimal Speed Advisory (GLOSA) system, the distance between the TL and the bicycle is derived from the GPS location of the bicycle and the location information received from the TL [24]. In addition, it gives an optimal recommended speed for the rider when approaching the traffic light. However, it may overwhelm the rider with excessive information and the rider is responsible for acknowledging and responding to this information, as the proposed system does not assist in adjusting the bicycle's speed.

Although GPS is widely available on all smartphones, sharing the location of cyclists might affect their privacy and make them vulnerable to malicious activities by tracking their movements and mobility history. To improve the

distance estimation accuracy using positional solutions, [21] have combined the Global Navigation Satellite System (GNSS), inertial and magnetic data using an extended Kalman filter to enhance bicycle localization in urban environments. However, this method requires additional computation and hardware, such as GPS equipment and Inertial measurement units on the bicycle. In addition, the TLs should also know their position information that is accessible to the GPS for accurately estimating the distance.

Another wireless solution proposed in [10] has used a combination of a log-normal shadowing model and an adaptive neural fuzzy inference system to reduce the distance estimation error between bicycles and anchor nodes. However, the computation and convergence time depend on a set of parameters, such as the number of membership functions, which is unsuitable for our application when the bicycle has to adapt its speed during a limited time window. Furthermore, several real-time applications use sensors like cameras, LiDAR, and ultrasonic to estimate the distance. However cameras and LiDAR are expensive, they could be affected by the environmental conditions and use high computational power in identifying the objects (in this case TL) that are required to estimate the distance. Meanwhile, [6] enabled cars to detect bicycles using Bluetooth beacons and trigger an alert to the driver when the cyclist is approaching closer to 50 m [6]. The path loss model and the Received Signal Strength Indicator (RSSI) of the received beacons enable the calculation of the distance. Yet, the distance estimation is not accurate enough due to reflection, and scattering, which brings distance estimation error and might affect the possibility of catching the green light in our application.

In this work, we aim to provide a low-cost solution for distance estimation for the long-rage application to 100 m, to avoid privacy issues presented when sharing the bicycles' GPS location, and dynamically enhance the RSSI-based distance estimation along the journey to cross the intersection.

## 3 System Modeling and Problem Formulation

In this section, we first explain the bicycle dynamics and the parameters used for the fuzzy logic controller. Then we will formalize the adaptation strategy as a convex optimization problem to smoothly adapt the bicycle's speed while preserving the cyclist's comfort and safety. In this paper, safety and comfort refer to maintaining acceleration and speed in a predefined range. This range might change according to the cyclist's preference and capabilities. However, to be able to assess our system we will consider safety by maintaining an acceleration in the range of [–0.4, 0.4 $m/s^2$] and a speed in the range of (16–20 km/h), as recommended in the literature [13].

### 3.1 System Modeling of Bicycle Dynamics

A bicycle in motion follows specific physics laws. The power required to move a bicycle with an expected velocity $v_{exp}$, has to deal with resisting forces. There

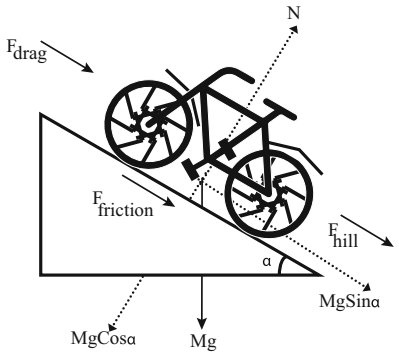


**Fig. 1.** Free-body diagram of all resisting environmental forces acting on a bicycle when moving uphill.

are three resisting forces as shown in Fig. 1: $F_{drag}$ air drag, $F_{hill}$ gradient drag, and $F_{friction}$ road surface friction at the point of contact on the ground.

The total power required, $P_{req}$, is the product of resisting force (sum of all resisting forces) and the expected velocity, $v_{exp}$ (since $Power = Force \times Velocity$):

$$P_{req} = (F_{drag} + F_{hill} + F_{friction}) \times v_{exp} \quad . \tag{1}$$

$F_{drag}$ is characterized by the atmospheric drag coefficient $C_d$, frontal area $A_c$, atmospheric density $\rho$, and bicycle's relative velocity to wind $v_{relative}$ (in our simulation the wind's velocity is negligible, hence this $v_{relative}$ eventually becomes $v_{curr}$):

$$F_{drag} = \frac{C_d\, A_c\, \rho}{2} \, (v_{relative})^2 \quad . \tag{2}$$

$F_{hill}$ is proportional to the object's mass $m$, gravitational force $g$, the angle of elevation/depression of the road surface $\alpha$:

$$F_{hill} = m\, g\, \sin\alpha \quad , \tag{3}$$

and $F_{friction}$ is governed by the friction coefficient $\mu$, the object's mass $m$, and gravitational force $g$ and the angle of elevation/depression of the road surface $\alpha$:

$$F_{friction} = m\, g\, \mu\, \cos\alpha \quad . \tag{4}$$

The total power provided to the bicycle's transmission system $P_{req}$ is the sum of the human pedal power and the motor power, which decides the current velocity of the bicycle $v_{curr}$.

$$P_{req} = P_{human} + P_{motor} \quad . \tag{5}$$

The current velocity of the bicycle $v_{curr}$ should reach the expected velocity $v_{exp}$ as close as possible under the influence of the controller. By substituting all

the resisting forces Eqs. (2) to (4) in Eq. (1) using Eq. (5) and rearranging, we can get

$$v_{curr} = \frac{P_{human} + P_{motor}}{F_{drag} + F_{hill} + F_{friction}} \quad . \tag{6}$$

This equation determines how much motor power should be provided by FLC to reach the expected velocity.

### 3.2 Problem Formulation of Bicycle Speed Adaptation

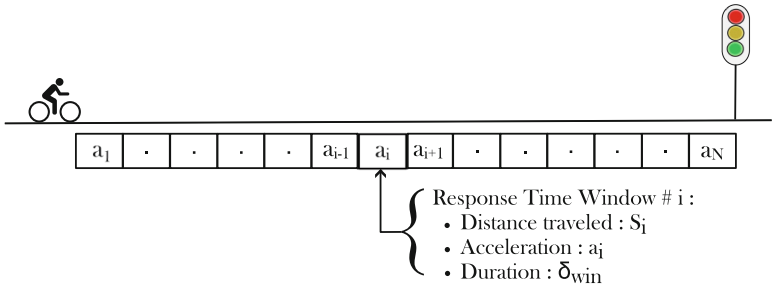


**Fig. 2.** Scenario representation where Time To Red is divided into $N$ equal Response Time Windows (RTW) of a duration $\delta_{win}$ each (Color figure online)

According to the bicycle dynamics in Sect. 3.1, we can control the motor power to reach any expected velocity when the human pedal power and environmental-related forces are known. However, the expected velocity is directly linked to the safety and comfort of cyclists. Therefore, our aim is to smoothly accelerate the bicycle, when the current velocity $v_{curr}$ is not sufficient to catch the green light while maintaining safety and comfort. In theory, deceleration is possible, but this work focuses solely on acceleration due to two reasons: i) We aim to retain human control and avoid complete system takeover. This means no motor assistance if there is no human pedal power. ii) Implementing deceleration alongside acceleration requires additional electronic blocks, which is beyond the scope of this work.

We formulate the problem as a convex optimization problem where we minimize the variance of the accelerations while: i) ensuring the possibility to catch the green light ii) not exceeding preset acceleration and velocity thresholds. The optimization problem can be expressed as follows:

$$\underset{a_i}{\text{argmin}} \quad \sum_{i=1}^{N} (a_i - \frac{1}{N} \sum_{j=1}^{N} a_j)^2 \quad , \tag{7}$$

$$\text{s.t.} \quad \sum_{i=1}^{N} S_i \geq D_{TL} \quad , \tag{8}$$

$$v_i \leq v_{max} \quad for \quad i \in [1....N] \quad , \tag{9}$$

$$0 \leq a_i \leq a_{max} \quad for \quad i \in [1....N] \quad . \tag{10}$$

As seen in Fig. 2, $S_i = v_{i-1}\,\delta_{win} + \frac{1}{2}\,a_i\,\delta_{win}^2$ is the distance traveled at the $i^{th}$ time window of a duration $\delta_{win}$, where $N = \lfloor \frac{TTR}{\delta_{win}} \rfloor$ represents the number of Response Time Windows (RTW) of the system, $v_{max}$ is the maximum allowed velocity, $a_{max}$ is the maximum acceleration that could be tuned by the cyclist according to his comfort and safety range, and $D_{TL}$ is the distance between the bicycle and the TL.

Once $a_i$ is calculated, we can derive $v_{exp,i}$ as follows:

$$v_{exp,i} = v_{exp,i-1} + a_i\,\delta_{win} \quad . \tag{11}$$

After getting the expected velocity, a controller shall supply the motor assistance with the required power to reach this expected velocity.

## 4 Methodology and System Design

This section introduces our system design and methodologies for solving the speed adaptation problem formulated in Sect. 3.2.

As shown in Fig. 3, the ISA consists of two parts: a Control Unit, and a FLC. The control units takes $TTR$ and the RSSI measurements received from the BLE module as input and estimates the distance to the TL and calculates the expected velocities. Then, the FLC estimates the required motor power to reach the expected velocity $v_{exp}$ to assist the rider in catching the green light. The expected velocity in this case is the required velocity to move the bicycle from one window to the other. One of the inputs to the FLC is the velocity error $v_{error}$, which is the difference between the expected velocity $v_{exp}$ to catch the green light and the bicycle's current velocity $v_{curr}$. The other input is the Human pedal power $P_{human}$. The $v_{curr}$ in practical can simply be achieved using a speed sensor in the bicycle, however for the simulation we realize this using Eq. (6). We will introduce the details of the control unit and the FLC in the following sub-sections.

### 4.1 Control Unit: Expected Velocity Calculation Based on Dynamic Distance Estimation Combining RSSI Path Loss Model with Kalman Filter

In this subsection, we introduce how we estimate the distance to the TL on the one hand and how we derive the expected velocity to catch the green light on the other hand.

The Control Unit, as shown in Fig. 4, extracts the RSSI measurements and the $TTR$ value from the BLE module and estimates the required acceleration to catch the green light. The distance estimation error is quite significant as the RSSI measurements fluctuate even when the bicycle is at the same distance from

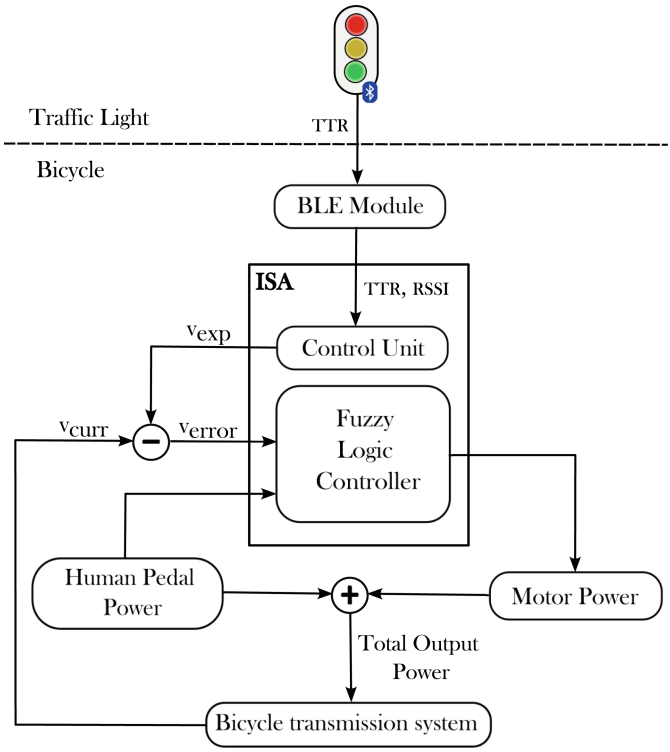


**Fig. 3.** Proposed communication-based ISA for e-bikes

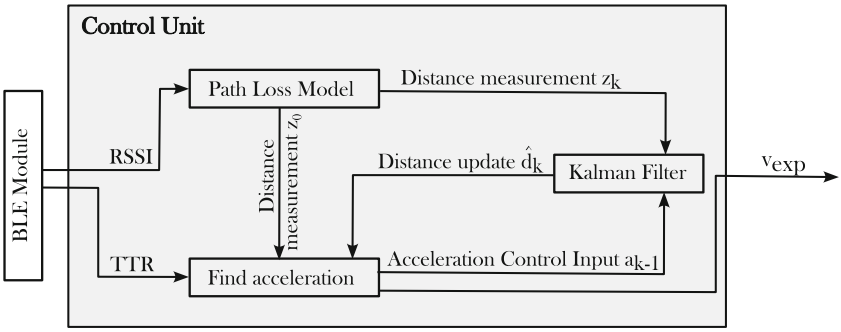


**Fig. 4.** Control Unit

the TL. Therefore, it affects the cyclist's comfort and the chance to catch the green light. To mitigate this issue, we apply a Kalman filter to enhance distance estimation accuracy while the bicycle is moving. The system state of the bicycle evolves from a previous state to the next state following Newton's law of motion and can be expressed as follows:

$$X_k = A\,X_{k-1} + B\,a_{k-1} + w_{k-1} \quad , \tag{12}$$

where $X_k = \begin{pmatrix} d_k \\ v_k \end{pmatrix}$, $d_k$ and $v_k$ are the distance and speed of the bicycle at time $k$, respectively. $A = \begin{pmatrix} 1 & -\delta_t \\ 0 & 1 \end{pmatrix}$, $B = \begin{pmatrix} -\frac{\delta_t^2}{2} \\ \delta_t \end{pmatrix}$, $\delta_t$ is the period of the distance measurement inputs to the Kalman filter, and $w_{k-1}$ is the uncertainty of the model with a covariance $Q$.

Additionally, the measurement $z_k$, is the measured distance based on the extracted RSSI values obtained using Eq. (15):

$$z_k = HX_k + u_k \tag{13}$$

Where $H = \begin{pmatrix} 1 & 0 \end{pmatrix}$ and $u_k$ is the measurement noise with variance $R$. According to Friis formula for free-space transmission [9], the distance can be calculated using the RSSI based on the log-distance model [14], as follows:

$$RSSI[dBm] = C - 10\,n\,\log_{10}(d) \tag{14}$$

Here $C$ is a constant, $n$ is the path loss exponent, and $d$ is the distance in meters between the transmitter and the receiver. Hence, we could derive the distance measurement between the TL and the bicycle from the equation as follows:

$$z_k = 10^{\frac{C - RSSI_k}{10n}} \tag{15}$$

Since both the system model and the measurements have noise, we could obtain the distance estimation using the KF equations in Eq. (16) to find the best trade-off between them.

$$\begin{aligned} \hat{X}_k^- &= A\,\hat{X}_{k-1}^- + B\,a_{k-1} \\ P_k^- &= A\,P_{k-1}\,A^T + Q \\ K_k &= P_k^- H^T (H P_k^- H^T + R)^{-1} \\ \hat{X}_k &= \hat{X}_k^- + K_k(z_k - H\hat{X}_k^-) \\ P_k &= (I - K_k H)\,P_k^- \end{aligned} \tag{16}$$

where $P_k$ denotes the a posteriori estimate covariance matrix. Then we find the distance estimate as:

$$\hat{d}_k = H\hat{X}_k \tag{17}$$

The details of dynamically updating the distance estimates through the Kalman filter are listed in Algorithm 1. Since the Kalman filter needs several measurements to converge, we split the duration of the entire journey into $Nu$ windows. Each window is of a period $\Delta_t = \frac{TTR}{N_u}$ (line 8). During the duration of $\Delta_t$ and at each $\delta_t$ seconds ($\delta_t \ll \Delta_t$), the TL sends a $\delta_t - periodic$ beacon containing a TTR value to the bicycle and the Kalman filter uses the distance measurements of the RSSI path-loss model and the control input acceleration to update

the distance estimation (line 21 to line 23). At the end of each period $\Delta_t$, we decrement the value of $TTR$ by $\Delta_t$ and calculate the list of accelerations and the corresponding expected velocities using the last distance update from the Kalman filter (line 24 to line 29). Here we mention that the initial list of accelerations is calculated using only the distance measured through the path-loss model at the reception of the first beacon (line 13 and line 14). Having in hand the list of expected velocities we move to the next section to explain how we use it in order to estimate the required motor power to assist the cyclist to catch the green light.

**Algorithm 1.** Intelligent Speed Adaptation

1: **Initialization:**
2: Inputs: $N_u$, $\delta_{win}$, $P_{human}$, $\alpha$
3: Output: $P_{motor}$
4: FLC ← Fuzzy simulation using membership functions
5: Power motor ← MotorPower(fuzzy simulation, $V_{error}$, $P_{human}$)
6: **Main:**
7: **while** a beacon is received & Traffic Light Phase is Green **do**
8: Calculate $\Delta_t = \frac{TTR}{N_u}$
9: Calculate $i = \lfloor \frac{\Delta_t}{\delta_{win}} \rfloor$
10: Calculate $N = \frac{TTR}{\delta_{win}}$
11: $Timer = \Delta_t$
12: Start $Timer$
13: Calculate the distance measurement input of the Kalman Filter $z$ using Equation (15)
14: Calculate $[a_1, ., a_N]$ and $[v_{exp,1}, ., v_{exp,N}]$ through Equation (7) and Equation (11) using $z$ as the distance to the traffic light ($D_{TL} = z$).
15: **if** $Timer == 0$ **then**
16: $TTR \leftarrow TTR - \Delta_t$
17: $Timer = \Delta_t$
18: Start $Timer$
19: **end if**
20: $k = 1$
21: **while** a beacon is received & Traffic Light Phase is Green **do**
22: Calculate the distance measurement input of the Kalman Filter $z$ through Equation (15) using the received $RSSI$
23: Calculate the Kalman filter distance update $\hat{d}$ through Equation (12) - Equation (17).
24: **if** $Timer == 0$ **then**
25: $TTR \leftarrow TTR - \Delta_t$
26: **if** $TTR <= 0$ **then**
27: break
28: **else**
29: Calculate $[a_{ki}, ., a_N]$ and $[v_{exp,ki}, ., v_{exp,N}]$ through Equation (7) and Equation (11) using the last updated $\hat{d}$ and $TTR$
30: Calculate $v_{curr}$ using Equations (2) to (4) and (6)
31: Calculate $v_{error} = v_{exp} - v_{curr}$
32: Calculate $P_{motor}$ using inputs $P_{human}$ & $v_{error}$ with FLC
33: $k \leftarrow k + 1$
34: $Timer = \Delta_t$
35: Start $Timer$
36: **end if**
37: **end if**
38: **end while**
39: **end while**

### 4.2 Fuzzy Logic Controller for Adapting the Speed

This sub-section explains how FLC controls the motor power to reach the expected velocity $v_{exp}$ obtained by the control unit above.

The FLC processes the inputs $v_{error}$ and $P_{human}$ in three stages: a) fuzzification, b) inference, and c) defuzzification, to estimate the motor power $P_{motor}$. In the fuzzification stage, crisp input values are transformed into fuzzy variables using the membership function (MF) shown in Fig. 5. Next, the fuzzy inference system (FIS) applies fuzzy rules and operators (e.g., AND, NOT, OR) from Table 1 to generate a new set of fuzzy variables. Finally, the FIS's fuzzy variables are converted back to crisp output values using centroid defuzzification. To maintain mathematical simplicity, the triangular membership function is utilized to prepare the MFs and linguistic variables with their abbreviations, all based on heuristic rules.

**Table 1.** Fuzzy inference rules for velocity error & human pedal power inputs and motor power output

| Velocity error ($v_{error}$) | Human pedal power ($P_{human}$) | | | |
|---|---|---|---|---|
| | VL | L | M | H |
| | | Motor | Power | ($P_{motor}$) |
| ***Z*** | VL | VL | L | L |
| ***VL*** | VL | L | L | M |
| ***L*** | VL | L | M | M |
| ***M*** | L | M | M | H |
| ***MH*** | L | M | H | H |
| ***H*** | M | M | H | VH |
| ***VH*** | H | H | VH | VH |

For the $v_{error}$, seven linguistic variables are created including **Zero (Z)**, **Very Low (VL)**, **Low (L)**, **Medium (M)**, **Medium High (MH)**, **High (H)**, and **Very High (VH)** Fig. 5 (a). Since regulations in the European Union require turning off the motor assistance when the velocity exceeds 25 km/h, the velocity error MF is thereby in the range of (0–25 km/h).

The human pedal power is represented by four linguistic variables: **Very Low (VL)**, **Low (L)**, **Medium (M)**, and **High (H)**. While Fig. 5 (b) shows the power range as (0–100) W, the MF can be dynamically adapted by adjusting the triangular center points to accommodate different power ranges exerted by cyclists. The human pedal power MF is constructed by adopting the slope gradient and corresponding human pedal power values from [13] as seen in Table 2. The slope gradient is between 0–3%, and their corresponding human pedal power is modeled from 45–125 W with distinct variances.

The motor power is represented by five linguistic variables: **Very Low (VL)**, **Low (L)**, **Medium (M)**, **High (H)**, and **Very High (VH)**, which define the

fuzzy sets of output motor power. As our approach utilizes Mamdani FIS, the output MF is constructed with fuzzy sets using if-then inference rules to handle uncertainties, as depicted in Table 1 [16].

Referring to [16], the construction of the 28 specified fuzzy rules in Table 1 involves a heuristic approach using the "Fuzzy AND" operator. The rules are as follows: First, when pedal power is constant, an increase in velocity error necessitates more motor power. Second, when velocity error is constant, an increase in pedal power also requires additional motor power. Third, the motor power should be reduced to zero when either human pedal power tends to zero or the current velocity exceeds 25 km/h. These rules determine the fuzzy output variable using the fuzzy max-min inference technique.

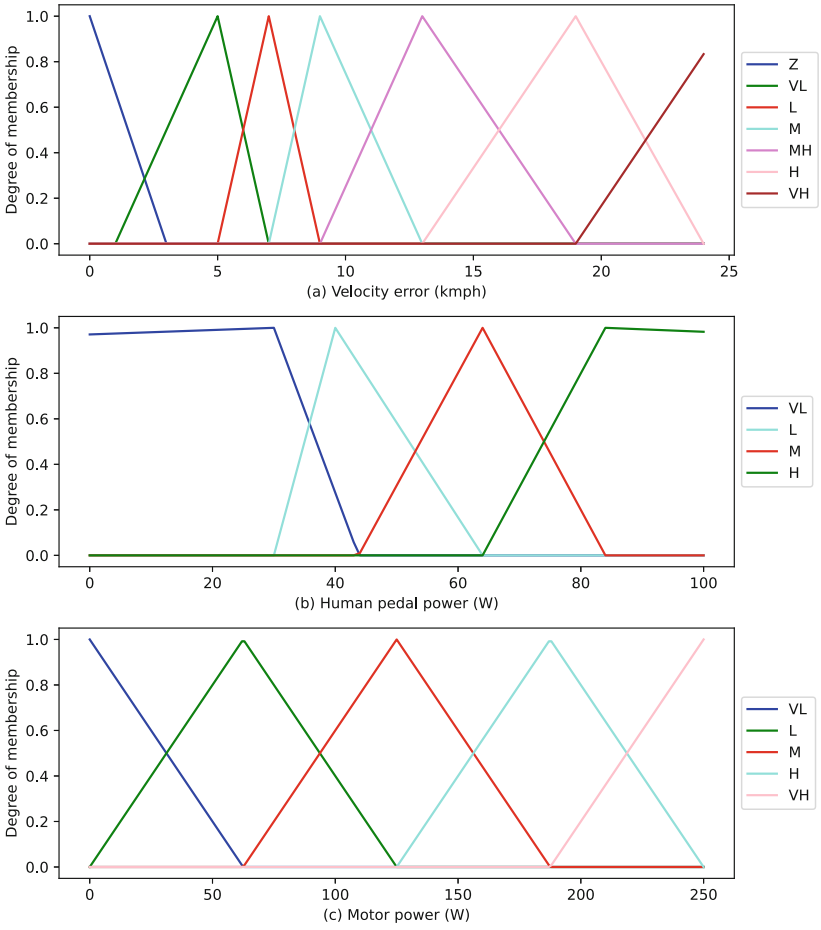


**Fig. 5.** FLC's linguistic variables and their associated membership functions for inputs a) Velocity error, (b) Human pedal power, and output (c) Motor power.

**Table 2.** Slope gradient and it's corresponding human pedal power

| Parameters | Slope grade | | | |
|---|---|---|---|---|
| | 0% | 1% | 2% | 3% |
| Total percent of individual slopes in the entire sampled slope data | 70% | 15% | 10% | 5% |
| Human pedal power mean and variance for different slope values | 45,30 | 65,40 | 95,50 | 125,60 |

## 5 Results

In this section, we simulate bicycle's dynamics and combine that with the implemented controller and samples taken from a large set of BLE propagation measurements. In addition, we evaluate the performance of ISA in terms of comfort, safety, and the chance to catch the green light. As explained previously, comfort and safety entail the preservation of acceleration and velocity within predetermined ranges. These ranges are guaranteed by the solution design through Eq. (10) and Eq. (9). The constant parameters required for simulation in the equations are given in Table 3.

**Table 3.** Simulation Parameters

| Conditions | Parameters | Value |
|---|---|---|
| ***Environmental*** | $C_d$ | *0.5* |
| | $A_c$ | *1* $m^2$ |
| | $\rho$ | *1.18* $kg/m^3$ |
| | $\mu$ | *0.014* |
| | $\alpha$ | *(0,1,2,3)%* |
| | $g$ | *9.8* $m/s^2$ |
| ***Rider*** | ***mass*** | 75 kg |
| | ***pedal power*** | *(0 - max W)* |
| ***Journey*** | $D_{TL,init}$ | 100 m |
| | $v_{init}$ | $v_{init} \in [10, 20] Km/h$ |
| | $TTR_{init}$ | $TTR \in [15, 25] s$ |
| | $v_{max}$ | 20 Km/h |
| | $a_{max}$ | $0.4 m/s^2$ |
| | $f_b$ | 4 Hz |
| | $\delta_{win}$ | 1 s |
| | $N_u$ | 4 |
| **Number of simulations** | – | $2^{15}$ |

### 5.1 Data Collection and Generation

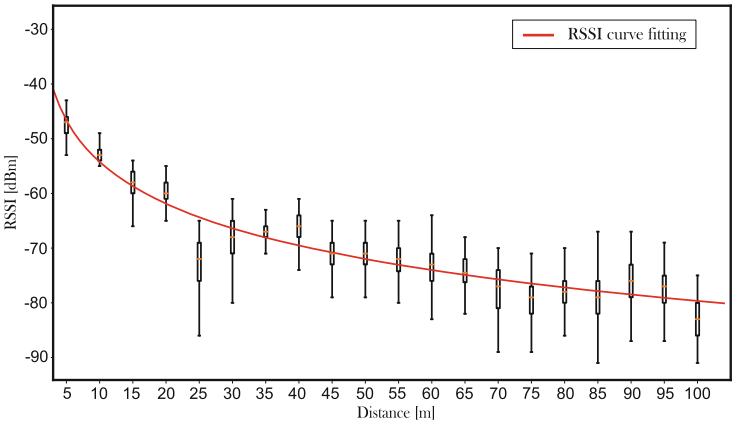


**Fig. 6.** RSSI Path Loss model with $n = 2.5$ and $C = -28.8$

We have collected RSSI measurements using two Nordic development kits NRF52832, one as a transmitter (Tx) and the other as a receiver (Rx). Both boards were running the BLE v5 protocol stack. Segger-embedded systems and C++ were used to program the two boards; one was configured as the BLE central device (Rx), and the other was configured as a peripheral device (Tx). The transmission power for the experiments has been set to 0 dBm. We have recorded the RSSI on the receiver side at each step of 5 m to a maximum distance of 100 m between the central and peripheral nodes. More than 150 packets containing RSSI values have been recorded at each step. In our setup, we assume that the roadside unit (in this case TL), Tx, will have a Line Of Sight (LOS) with the On-Board Unit (OBU), Rx, on the bicycle. Therefore, we ensured a clear LOS between Tx and Rx in the experimental measurements. One major motivation behind this assumption is that in many European countries, such as the Netherlands, the separation between bicycle lanes and car lanes is widely considered for safety, so the LOS is less to be obstructed by obstacles such as cars and trucks. After fitting the data curve, as shown in Fig. 6, we obtain from Eq. (15): $C = -28.8$ and the path loss exponent $n = 2.5$. These values depend on the measured environment and we assume that during equipping the TLs with BLE modules calibrations have to be done.

Furthermore, we have synthetically generated the slope and human pedal power data, for the simulation, provided in [13]. The slope values are in the range (0–3%). This means increase in the road's gradient, in meters, over a horizontal run of 100 m. For example, a 2% slope constitutes a rise of 2 m over a distance of 100 m. The slope generation involves uniform distribution for respective slope values as shown in Table 2 along with an additive white Gaussian noise of mean

and standard deviation 0 and 0.2 to resemble the real world road profile. The generation of human pedal power corresponding to the slope involves using a normal distribution with mean and variance values listed in e.g., a slope of 0% will have 70% of the total distribution Table 2.

### 5.2 Impacts of Distance Estimation Error on ISA

To evaluate the distance estimation accuracy, we have generated many scenarios of journeys. Each journey starts when the bicycle receives the first beacon and ends when it reaches the TL. At the start of each journey, we randomly generate an initial velocity $v_{init}$ and $TTR_{init}$ value as mentioned in Table 3, where *init* refers to the value at the reception of the first beacon.

To calculate the distance estimation error, we first obtain the real distance of the bicycle to TL along the journey. It is calculated by first solving the optimization problem in Eq. (7), to obtain a list of accelerations assuming that the initial distance to the traffic light is known; then we get the real distance of the bicycles at every second through Newton's law of motion. Further, at each distance of 5 meters, we compare the estimated distances of the Kalman Filter and the Path Loss model to the real distance between the bicycle and the TL. The RSSI values are fed to the Control Unit at a frequency of $f_b = 4\,\text{Hz}$. As we collected the RSSI values only at discrete points of every 5 m, we randomly select one RSSI value from the set of collected data that is closest to the current position of the bicycle.

In Fig. 7, we show the Mean Absolute Error (MAE) of the estimated distance of Kalman filter and path-loss model. The mean is calculated over $2^{15}$ combinations of initial velocities, $TTR$, road slopes, and human pedal power. As expected, the Kalman filter has less MAE than the Path-loss model, as we are reducing the noise coming from the RSSI measurements. Due to the fact that our RSSI collected data is only done at each distance of 5 m, in Fig. 6, we are losing accuracy of at least 2.5 m for the distance estimation. Therefore, collecting RSSI data at several different distances will give us better distance estimation accuracy.

To give a more straightforward illustration of the distance estimation, we show in Fig. 8 one scenario where $v_{init} = 15.47\,\text{km/h}$ and $TTR_{init} = 21.58\,\text{s}$. We have simulated this scenario for multiple runs considering the random selection of the RSSI measurements from the corresponding distances. At each second, we average all the estimated distances and compare those mean values of Kalman Filter and Path Loss model with the real distances. The results are consistent with Fig. 7 that ISA method is closer to the optimal solution and less fluctuating than using only Path Loss model for distance estimation.

### 5.3 ISA Performance Evaluation Based on Success Percentage of Catching the Green Light

We have evaluated our system based on the percentage of scenarios where we successfully catch the green light. We have generated random values of initial

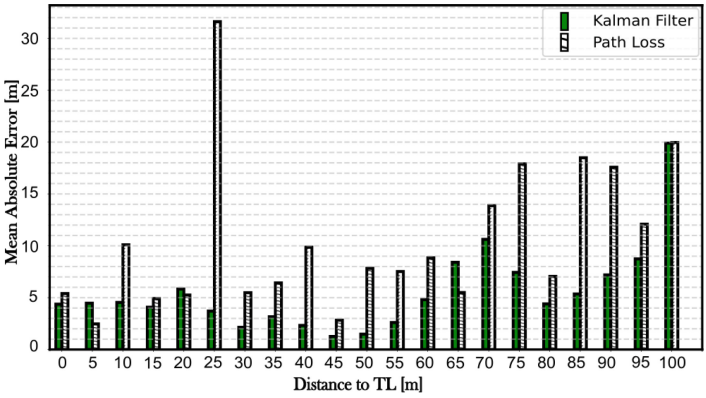


**Fig. 7.** Mean Absolute Error of Distance Estimation.

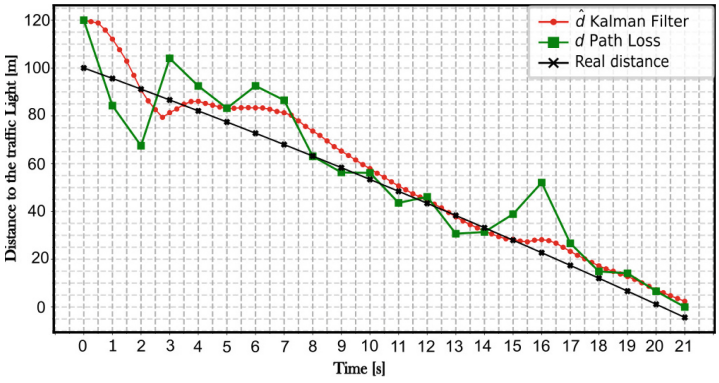


**Fig. 8.** Average Estimated distances using Kalman Filter and Path Loss model compared to real distances to the TL through one journey with $v_{init} = 15.47\,\text{km/h}$ and $TTR_{init} = 21.58\,\text{s}$

velocities in the range of [10, 20] km/h and initial $TTR_{init}$ in the range of [15, 25] s. Then we defined $2^{15}$ combinations of initial velocities, initial TTRs, road slopes and human pedal power. Each combination defines one scenario. The rest of the simulation parameters can be found in Table 3. Furthermore, due to the formulation of convex optimization problem the control unit ensures the safety and comfort metrics. It is prepared to satisfy the upper and lower inequality constraints presented in Eq. (7).

In Table 4, we illustrate a range of techniques alongside their respective success rates in capturing the green light. It is essential to note that the success rates in this analysis are derived from a subset comprising 57.80% of the $2^{15}$ simulation scenarios wherein catching the green light is physically feasible. Regarding the initial scenario, where the bicycle maintains a constant speed without any

**Table 4.** The percentage of success in catching green light

| Method | Success percentage |
|---|---|
| Without speed adaptation | 37.54% |
| Speed adaptation with Path Loss model | 60% |
| ISA | 66.40% |

adjustments, the success rate is recorded at 37.54%, indicating the lowest success rate among the techniques considered.

Comparatively, the Intelligent Speed Adaptation (ISA) method demonstrates a notable 66.40% probability of catching the green light, marking a significant enhancement of nearly 77% compared to the non-adaptive approach. Moreover, this improvement is approximately 10% relative to that achieved through the implementation of the path-loss model, attributable to the more accurate distance estimations provided by the ISA methodology. Attaining a flawless success rate hinges on the system's ability to obtain precise distance estimates to the traffic light and promptly adjust the speed upon receiving the first beacon. However, our system relies on obtaining additional beacons during the journey to refine the distance estimation to the traffic light, enabling the calculation of the necessary acceleration for intercepting the green light.

## 6 Discussion and Future Work

This work serves as a starting point in the design of smart bicycles for self-speed adaptation to assist cyclists in catching the green light. There are, however, several aspects that need to be investigated in the future. In particular, we anticipate continuing our research work along the following lines.

- ***Deceleration and large-scale evaluation.*** As a proof-of-concept, ISA is evaluated when there is only one bicycle that needs to accelerate to catch a traffic light. We need to further investigate how to decelerate and how to quantify the impacts of other road users on the speed adaptation. To include both acceleration and deceleration in one system will increase the complexity, and hence we first focused only on acceleration. In addition, physical implementation with embedded systems is needed to test the system in the real traffic scenarios. Time and battery consumption saved will be further used to evaluate the system when there are multiple traffic lights along the journey.
- ***Interaction with smart traffic lights.*** The results showed in this paper are based on a normal traffic light with fixed signal phase and timing (SPaT). Smart traffic lights are able to change the SPaT according to the traffic situations. Nevertheless, we believe that the basic building blocks of ISA are well posed to tackle the dynamical SPaT because of two reasons. First, ISA can obtain the new SPaT information based on the periodically received BLE beacons; and second, ISA dynamically estimates the distance to the traffic

light along the journey and updates the control policy accordingly. We need to generate different scenarios to test this functionality and evaluate the effectiveness in the next step.

## 7 Conclusion

This paper proposes an intelligent speed adaptation system at traffic lights for cyclists to increase the chances of catching the green light. The system combines BLE communication with FLC based motor power control and can be fully implemented on the bicycle. It overcomes the limitations of existing methods in two ways: first, compared with smart traffic lights that adapt signal phase to prioritize a group of cyclists conditionally, ISA provides personalized assistance considering the cyclist's velocity, pedal power, distance to the traffic light, time to red, and slopes of roads; second, compared with smartphone application systems that adapt to traffic lights, ISA does not leak users' private information to third parties. Extensive simulation results show that our system improves the probability of catching a green light by 77% compared to no speed adaptation while maintaining the safety and comfort of the cyclist.

## References

1. Enschede Cycling App - Enschede Cycling City. https://enschedefietsstad.nl/enschede-fietst-app/
2. Intelligent Traffic Light Installations — Rijkswaterstaat. https://www.rijkswaterstaat.nl/en/mobility/smart-mobility/talking-traffic/intelligent-traffic-light-installations
3. PrioBike-HH: Enhancing cycling comfort and safety in Hamburg, Interreg VB North Sea Region Programme. https://northsearegion.eu/bits/news/priobike-hh-enhancing-cycling-comfort-and-safety-in-hamburg/
4. Schwung - Lekker snel door groen. https://schwung.nu/
5. Abagnale, C., Cardone, M., Iodice, P., Strano, S., Terzo, M., Vorraro, G.: Model-based control for an innovative power-assisted bicycle. Energy Procedia **81**, 606–617 (2015). https://doi.org/10.1016/J.EGYPRO.2015.12.045
6. Anaya, J.J., Talavera, E., Gimenez, D., Gomez, N., Felipe, J., Naranjo, J.E.: Vulnerable road users detection using V2X communications. In: IEEE Conference on Intelligent Transportation Systems, Proceedings, ITSC, vol. 2015-Octob, May 2020, pp. 107–112 (2015). https://doi.org/10.1109/ITSC.2015.26
7. Bopp, M., Sims, D., Piatkowski, D.: Bicycling for transportation: an evidence-base for communities. Bicycling for Transportation: An Evidence-Base for Communities, pp. 1–227 (2018). https://doi.org/10.1016/C2016-0-03936-0
8. Chen, P.H.: Intelligence application: elebike fuzzy control Part I. In: Proceedings of the 7th International Conference on Machine Learning and Cybernetics, ICMLC, vol. 6, pp. 3581–3585 (2008). https://doi.org/10.1109/ICMLC.2008.4621025
9. Friis, H.T.: A note on a simple transmission formula. Proc. IRE **34**(5), 254–256 (1946). https://doi.org/10.1109/JRPROC.1946.234568

10. Gharghan, S.K., Nordin, R., Jawad, A.M., Jawad, H.M., Ismail, M.: Adaptive neural fuzzy inference system for accurate localization of wireless sensor network in outdoor and indoor cycling applications. IEEE Access **6**, 38475–38489 (2018). https://doi.org/10.1109/ACCESS.2018.2853996
11. Gojanovic, B., Welker, J., Iglesias, K., Daucourt, C., Gremion, G.: Electric bicycles as a new active transportation modality to promote health. Med. Sci. Sports Exerc. **43**(11), 2204–2210 (2011). https://doi.org/10.1249/MSS.0B013E31821CBDC8
12. Guarisco, M., Gao, F., Paire, D.: Autonomy and user experience enhancement control of an electrically assisted bicycle with dual-wheel drive. In: IEEE Industry Application Society - 51st Annual Meeting, IAS 2015, Conference Record, December 2015. https://doi.org/10.1109/IAS.2015.7356842
13. Hsu, R.C., Liu, C.T., Chan, D.Y.: A reinforcement-learning-based assisted power management with QoR provisioning for human-electric hybrid bicycle. IEEE Trans. Ind. Electron. **59**(8), 3350–3359 (2012). https://doi.org/10.1109/TIE.2011.2141092
14. Ivanic, M., Mezei, I.: Distance estimation based on RSSI improvements of orientation aware nodes. In: 2018 Zooming Innovation in Consumer Technologies Conference, ZINC 2018, pp. 140–143, August 2018. https://doi.org/10.1109/ZINC.2018.8448660
15. Latham, A., Wood, P.R.: Inhabiting infrastructure: exploring the interactional spaces of urban cycling. Environ Plan A **47**(2), 300–319 (2015). https://doi.org/10.1068/A140049P
16. Lee, J.S., Jiang, J.W.: Enhanced fuzzy-logic-based power-assisted control with user-adaptive systems for human-electric bikes. IET Intell. Transp. Syst. **13**(10), 1492–1498 (2019). https://doi.org/10.1049/IET-ITS.2019.0092
17. Lee, J.S., Jiang, J.W., Sun, Y.H.: Design and simulation of control systems for electric-assist bikes. In: Proceedings of the 2016 IEEE 11th Conference on Industrial Electronics and Applications, ICIEA 2016, pp. 1736–1740, October 2016. https://doi.org/10.1109/ICIEA.2016.7603866
18. Liang, C.Y., Lin, W.H., Chang, B.: Applying fuzzy logic control to an electric bicycle. In: First International Conference on Innovative Computing, Information and Control 2006, ICICIC'06, pp. 513–516 (2006). https://doi.org/10.1109/ICICIC.2006.54
19. Lomonova, E.A., Vandenput, A.J., Rubáček, J., D'Herripon, B., Roovers, G.: Development of an improved electrically assisted bicycle. In: Conference Record - IAS Annual Meeting (IEEE Industry Applications Society), vol. 1, pp. 384–389 (2002). https://doi.org/10.1109/IAS.2002.1044116
20. Masatoku, K.: Regulations on electric bicycles in Japan. In: Proceedings of the Conference of Safety Popularization Electric Assist Bicycles, pp. 1–5 (2001)
21. Perul, J., Renaudin, V.: BIKES: bicycle itinerancy Kalman filter with embedded sensors for challenging urban environment. IEEE Sens. J. **22**(6), 5270–5277 (2022). https://doi.org/10.1109/JSEN.2021.3086004
22. Romanillos, G., Gutiérrez, J.: Cyclists do better. Analyzing urban cycling operating speeds and accessibility. Int. J. Sustain. Transp. **14**(6), 448–464 (2020). https://doi.org/10.1080/15568318.2019.1575493
23. Indulal, S., Chandramohanan Nair, P.S.: A novel approach in automatic control of a Hybrid Bicycle — IET Conference Publication — IEEE Xplore (2007)
24. Tal, I., Ciubotaru, B., Muntean, G.M.: Vehicular-communications-based speed advisory system for electric bicycles. IEEE Trans. Veh. Technol. **65**(6), 4129–4143 (2016). https://doi.org/10.1109/TVT.2015.2442338